Received: 14 August 2020 | Revised: 27 August 2020 | Accepted: 29 August 2020

DOI: 10.1002/aoc.6008

Applied Organometallic Chemistry WILEY

FULL PAPER

Evaluation and comparison of ^{99m}Tc-labeled D-glucosamine derivatives with different ^{99m}Tc cores as potential tumor imaging agents

Xuran Zhang | **Qianqian Gan** | **Qing Ruan** | **Di Xiao** | **Junbo Zhang**

Key Laboratory of Radiopharmaceuticals of Ministry of Education, College of Chemistry, Beijing Normal University, Beijing, 100875, China

Correspondence
Junbo Zhang, Key Laboratory of Radiopharmaceuticals of Ministry of Education, College of Chemistry, Beijing Normal University, Beijing 100875, China.
Email: zhjunbo@bnu.edu.cn

Funding information
China Postdoctoral Science Foundation, Grant/Award Number: 212400211; Beijing Municipal Science and Technology Commission, Grant/Award Number: Z181100002218033; National Natural Science Foundation of China, Grant/Award Number: 21771023

Isocyanide is a strong coordination ligand that can coordinate with $[^{99m}Tc(I)(CO)_3]^+$ core and $[^{99m}Tc(I)]^+$ core to produce stable ^{99m}Tc complexes, therefore developing a ^{99m}Tc-labeled isocyanide complex for single-photon emission computed tomography (SPECT) imaging is considered to be of great interest. In order to develop potential tumor imaging agents with satisfied tumor uptake and suitable pharmacokinetic properties in vivo, a novel D-glucosamine isocyanide derivative, 4-isocyano-*N*-(2,4,5-trihydroxy-6-(hydroxymethyl)tetrahydro-2*H*-pyran-3-yl)butanamide (CN3DG), was synthesized and radiolabeled with $[^{99m}Tc(I)]^+$ and $[^{99m}Tc(CO)_3]^+$ cores to obtain $[^{99m}Tc(CN3DG)_6]^+$ and $[^{99m}Tc(CO)_3(CN3DG)_3]^+$ in high radiolabeling yields (>95%). Both of the complexes showed good hydrophilicity and great stability in vitro. Cell uptake studies performed in S180 cells demonstrated they were transported into cells by glucose transporters. Biodistribution studies of the two complexes in mice bearing S180 tumor showed they had high tumor uptakes and rapid clearance from muscle and blood so that the tumor/blood and tumor/muscle ratios were high. By comparison, $[^{99m}Tc(CN3DG)_6]^+$ was superior to $[^{99m}Tc(CO)_3(CN3DG)_3]^+$ in regard to tumor uptake, tumor/blood and tumor/liver ratios. S180 tumors could be seen clearly from the SPECT/CT images with $[^{99m}Tc(CN3DG)_6]^+$. Considering its favorable properties, $[^{99m}Tc(CN3DG)_6]^+$ would be a promising tumor imaging agent and needs to be further studied.

KEYWORDS

D-glucosamine, isocyanide, radiopharmaceutical, SPECT, tumor imaging

1 | INTRODUCTION

As cancer is becoming the leading disease that threatens people's health and lives, early diagnosis of cancers plays an important role in preventing their progression and making treatment options personally. Positron emission tomography (PET) and single-photon emission computed tomography (SPECT) are the main noninvasive nuclear imaging modalities that used in cancer diagnosis, staging and monitoring the chemotherapy response.[1,2] 2-[^{18}F]Fluoro-2-deoxy-D-glucose (^{18}F-FDG) is a widely used PET tracer for clinical tumor imaging due to its similar chemical structure to glucose that can be recognized by glut transporters (GLUTS) and transported into cancer cells.[3–6] However, the short half-life ($T_{1/2}$ = 110 min) of ^{18}F and its expensive production cost by a cyclotron limited its wide application.

Technetium-99m accounts for about 90% SPECT imaging studies in the world because of its suitable nuclide properties ($T_{1/2}$ = 6.02 h, E_γ = 140 keV) and

inexpensive diagnostic cost. Recently, many ^{99m}Tc-labeled glucose derivatives have been developed and evaluated as tumor imaging agents.[7–17] Among them, ^{99m}Tc-ethylenedicysteine-deoxyglucose (^{99m}Tc-ECDG) is the most promising metabolic imaging agent and is ongoing its phase III study.[18–20] However, the tumor/blood ratio of ^{99m}Tc-ECDG in A549 tumors was not satisfactory owing to its high blood uptake and slow clearance.

In our previous studies, a glucose derivative with an isonitrile group (CN5DG) was synthesized and radiolabeled with $[^{99m}Tc(I)]^+$ core to prepare ^{99m}Tc-CN5DG.[21] ^{99m}Tc-CN5DG exhibited a certain tumor uptake and favorable blood and muscle clearance; however, its tumor uptake needs to be increased, and its initial blood uptake needs to be decreased to obtain better SPECT images. Bearing in mind the different ^{99m}Tc cores, lipophilicity and overall size are the main factors influencing the biodistribution results of the resulting ^{99m}Tc complexes[22–26]; in this study, 4-isocyano-*N*-(2,4,5-trihydroxy-6-(hydroxymethyl)tetrahydro-2*H*-pyran-3-yl)butanamide (CN3DG) (Scheme 1) with less methylene number was synthesized and radiolabeled with $[^{99m}Tc(I)]^+$ core and $[^{99m}Tc(I)(CO)_3]^+$ core to obtain $[^{99m}Tc(CN3DG)_6]^+$ and $[^{99m}Tc(CO)_3(CN3DG)_3]^+$ (Figure 1). The feasibility of $[^{99m}Tc(CN3DG)_6]^+$ and $[^{99m}Tc(CO)_3(CN3DG)_3]^+$ as tumor imaging agents were evaluated and compared in rodents in this paper.

2 | EXPERIMENTAL SECTION

2.1 | Materials and methods

All chemical reagents and solvents were purchased from commercial companies and were used directly. $^{99m}TcO_4^-$ was obtained from a ^{99}Mo/^{99m}Tc generator. ^{1}H-NMR and ^{13}C-NMR data were acquired on a Bruker spectrometer (Avance 500, 400 MHz, USA). The MS spectrum was recorded on a Bruker solariX ESI mass spectrometer. Radiochemical purity was analyzed by HPLC equipped with a Waters 2489 UV system and a Gabi raytest radioactivity detector using an analytical column (18C, Kromasil, 100–5 μm, 250 × 4.6 mm). The HPLC gradient elution method: System 1 (A, 0.1% trifluoroacetate in water; B, 0.1% trifluoroacetate in acetonitrile) was 0–2 min, 10% B; 2–10 min, 10–90% B; 10–15 min, 90% B; 15–20 min, 90–10% B. System 2 (A, 0.1% trifluoroacetate in water; B, 0.1% trifluoroacetate in methanol) was 0–2 min, 10% B; 2–10 min, 10–90% B; 10–15 min, 90% B; 15–20 min, 90–10% B. Radioactivity (CPM) was recorded on a WIZARD$^{2®}$ 2480 PerkinElmer system. SPECT/CT images were acquired on a Trifoil Imaging Triumph Scanner (Triumph SPECT/CT, console-gr157). Animal studies were carried out in compliance with the Regulations on Laboratory Animals of Beijing Municipality and the guidelines of the Ethics Committee of Beijing Normal University.

2.2 | Chemistry and radiochemistry

2.2.1 | 6-Isocyano-*N*-(2,4,5-trihydroxy-6-(hydroxymethyl)tetrahydro-2*H*-pyran-3-yl)hexanamide (CN3DG, 5)

First, compound **4** was synthesized according to the published literature,[21] and the synthetic route was shown in Scheme 1. CN3DG (**5**) was synthesized as follows: D-glucosamine hydrochloride (117 mg, 0.54 mmol) and sodium hydroxide (22 mg, 0.54 mmol) were dissolved in methanol (20 ml) and stirred at room temperature for 30 min. To this stirred mixture, **4** (156 mg, 0.60 mmol) was added and the reaction mixture continued to stir at room temperature overnight. The solvent was removed under reduced vacuum, and the residue was washed with acetonitrile to obtain the crude product; then, silica gel column chromatography was used to obtain compound **5** as a white powder (85 mg, 57%). IR (KBr)/cm^{-1}: 3294.56 (—OH), 2148.79 (—NC), 1645.35 (—C═O). ^{1}H-NMR(400 MHz, D_2O): δ (ppm) 3.59–3.77 (m, 5*H*), 3.31–3.42 (m, 4*H*), 2.31–2.35 (m, 2*H*), 1.85 (s, 2*H*). ^{13}C-NMR (100 MHz, D_2O) δ 175.74, 175.52, 151.53 (t, J = 7 Hz, NC), 94.95, 90.85, 75.94, 73.81, 71.58, 70.65,

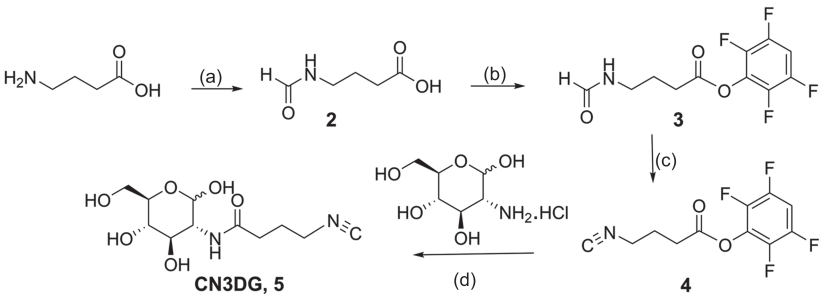

SCHEME 1 Synthesis of CN3DG. (a) DMF, formic acid, reflux; (b) 2,3,5,6-tetrafuorophenol, EDCI, CH_2Cl_2, rt; (c) Burgess reagent, CH_2Cl_2, rt; and (d) sodium hydroxide, CH_3OH, rt

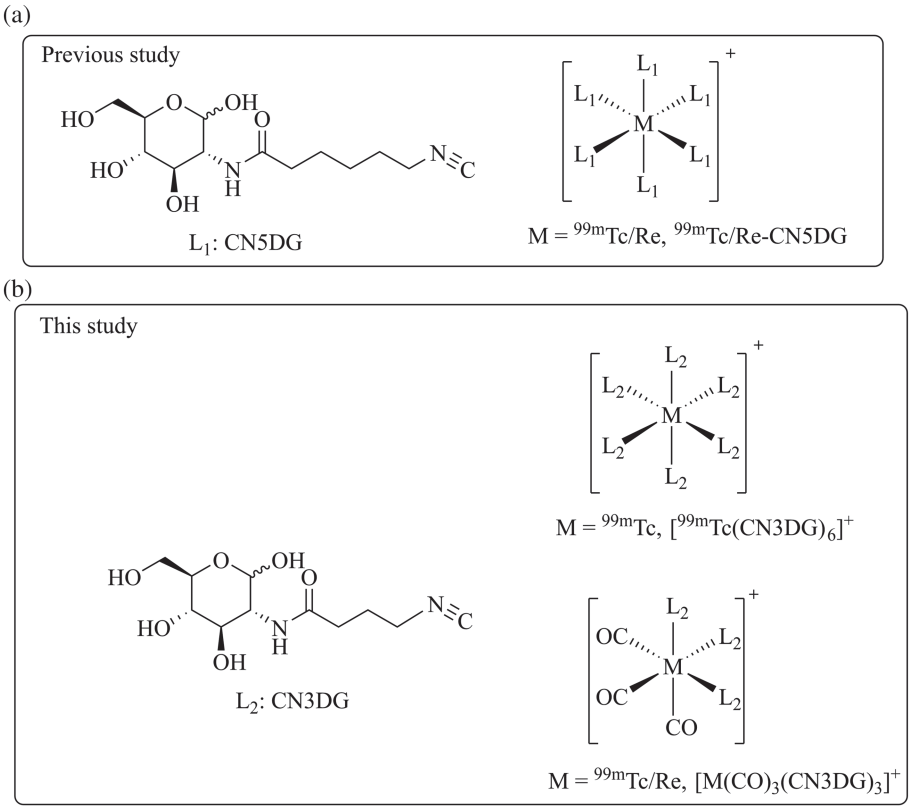

FIGURE 1 Chemical structures of CN5DG and CN3DG and their corresponding metal complexes

70.14, 69.94, 60.76, 60.61, 56.59, 54.34, 54.05, 40.93 (t, J = 6 Hz, NCH_2), 32.58, 32.41, 24.67, 24.58. HRMS (ESI): $[C_{11}H_{18}N_2O_6Na]^+$: *m/z* calcd. for $[M + Na]^+$ 297.1057, found 297.1052.

2.2.2 | Preparation of $[Re(CO)_3(CN3DG)_3]^+$

$[Re(CO)_3(CN3DG)_3]^+$ was synthesized according to the previous literature.[26] $[Re(CO)_5]Br$ (10 mg) was dissolved in 5 ml of purified water in a 10-ml penicillin vial, and the mixture was heated at 100°C overnight to obtain the intermediate $[Re(CO)_3(H_2O)_3]^+$. Then, 0.5 ml of the above mixture was added to a 10-ml penicillin vial, and CN3DG (50 mg) was added and heated at 100°C for 3 h. After cooling to room temperature, $[Re(CO)_3(CN3DG)_3]^+$ was purified by HPLC using System 1. ^{1}H-NMR (400 MHz, D_2O): δ (ppm) 3.54–3.82 (m, 21*H*), 3.23–3.47 (m, 6*H*), 2.23–2.42 (m, 6*H*), 1.87–2.01 (m, 6*H*). HRMS (ESI): $[Re(C_{11}H_{18}N_2O_6)_3(CO)_3]^+$: *m/z* calcd. for $ReC_{36}H_{54}N_6O_{21}$ 1093.2896, found 1093.2891.

2.2.3 | Radiolabeling

For preparation of $[^{99m}Tc(CN3DG)_6]^+$, to a 10-ml penicillin vial containing sodium citrate (1 mg) and L-cysteine (0.5 mg), 30-μl $SnCl_2{\cdot}2H_2O$ (1 mg ml^{-1}) were added. The pH value of the solution was adjusted to 5–6 by using 0.1 M NaOH. CN3DG (1 mg) and $^{99m}TcO_4^-$ (1–10 mCi) were then added, successively. The vial was sealed and heated at 100°C for 20 min. After cooling to room temperature, 10 μl of the labeling solution was injected into a radio-HPLC system for radiochemical purity determination (System 2).

For the preparation of $[^{99m}Tc(CO)_3(CN3DG)_3]^+$, $[^{99m}Tc(CO)_3(H_2O)_3]^+$ was firstly synthesized as radiolabeling intermediate according to the published literature.[26] The pH value of the intermediate was adjusted to 7–8 by using 1 M HCl, and it was added to a penicillin vial containing 1-mg CN3DG. The sealed vial was heated at 100°C for 20 min. After cooling to room temperature, 10 μl of the labeling solution was injected into a radio-HPLC system for radiochemical purity determination (System 1).

2.3 | Water/*n*-octanol partition coefficient determination

$[^{99m}Tc(CN3DG)_6]^+$ and $[^{99m}Tc(CO)_3(CN3DG)_3]^+$ separated from the HPLC system were used for partition coefficient determination. The separated complexes were concentrated in vacuo to remove the organic solvent and then 50 μl of each sample (1.85 MBq) was added to an

equal volume mixture (2 ml:2 ml) of PBS (0.1 M, pH 7.4) and *n*-octanol. The mixed solution was vortexed for 5 min and left to stand for 2 min, then the mixture was centrifuged for 5 min at 2000 rpm. Three samples (100 μl for each) from each layer were collected, and the radioactivity was measured on an automatic γ-counter. The partition coefficient (P) was calculated as follows: P = (radioactivity in octanol/radioactivity in aqueous layer). The partition coefficient (Log P) was reported as average of three experiments ± standard deviation (SD).

2.4 | Stability studies in vitro

Stability studies for each radiolabeled complex separated by the HPLC were carried out in saline and mice serum in vitro. Fifty microliters of each complex (370 kBq) was mixed with 1 ml of saline or 500 μl of freshly prepared mice serum. After 6 h in saline, 10 μl of each complex was analyzed by radio-HPLC for radiochemical purity determination ($n = 3$). For HPLC analysis of samples in mice serum for 2 h, 300 μl of acetonitrile was added into 200 μl of the incubated serum to precipitate the protein. After being centrifuged at 10,000 *g* for 5 min, the supernatant was collected and concentrated, and the remaining solution was analyzed with the radio-HPLC system.

2.5 | Cell uptake studies

The cell uptake blocking studies were conducted according to the previous published literatures.[20,21] S180 cells were used for cell uptake studies; 3×10^6 cells were suspended in 0.5 ml of glucose-free medium containing D-glucose (2 mg) or L-glucose (2 mg) (each group has five tubes) in 2-ml centrifuge tubes. Then, $[^{99m}Tc(CN3DG)_6]^+$ (0.5 ml, 740 kBq) or $[^{99m}Tc(CO)_3(CN3DG)_3]^+$ (0.5 ml, 740 kBq) was added, and the mixtures were incubated at 37°C for 4 h. After 4-h incubation, the tubes were centrifuged and the supernatant were removed. The precipitated cells were washed with cold phosphate-buffered saline (pH 7.4, 0.1 M) twice (2 × 1 ml), and the cell uptake radioactivity was measured by a γ-counter (PerkinElmer, WIZARD 2480).

2.6 | Biodistribution studies

Biodistribution data were collected according to the published literature.[22] Kunming female mice bearing S180 tumors (0.5–1.0 cm in diameter) were injected 74 kBq of ^{99m}Tc-labeled complexes ($[^{99m}Tc(CN3DG)_6]^+$ or $[^{99m}Tc(CO)_3(CN3DG)_3]^+$) via the tail vein. The animals were sacrificed at 0.5, 1, and 2 h post injection ($n = 5$). The interested organs were removed and weighted, and the radioactivity was collected on a gamma counter. The results were presented as the percentage of the injected dose per gram (%ID g^{-1}). The data were expressed as average ± SD of five animals.

2.7 | SPECT/CT imaging

A total of 0.1–0.2 ml of $[^{99m}Tc(CN3DG)_6]^+$ (74 MBq) was injected into S180 tumor-bearing mice via the tail vein ($n = 3$) and imaged at 0.5, 1, and 2 h post injection. For $[^{99m}Tc(CO)_3(CN3DG)_3]^+$, animals were imaged at 1 h post injection. The animals received a standard SPECT/CT protocol (MMP919 collimator, 20 min of SPECT scan followed by 4 min of CT scan) and being anesthetized with 1.5% isoflurane during the process. The SPECT/CT images were reconstructed by a HiSPECT software and analyzed with VivoQuant 2.5 software.

2.8 | Statistical analysis

The cell uptake data and the biodistribution data were calculated and analyzed with Microsoft Excel and Prism 5.01. All data were presented as average ± SD. To compare differences between two data, the Student's *t* test was used. $P < 0.05$ indicated a statistically significant difference.

3 | RESULTS AND DISCUSSION

3.1 | Chemistry and radiolabeling chemistry

CN3DG was prepared by reacting D-glucosamine hydrochloride with isonitrile bearing activated ester (**4**) under alkaline conditions (Scheme 1) overnight. In the last step, **4** was 1.2 times more than D-glucosamine hydrochloride to make D-glucosamine hydrochloride react completely. The excessive ester **4** could be removed easily by washing with acetonitrile. The chemical structure of CN3DG was confirmed by ^{1}H-NMR, ^{13}C-NMR, IR, and HRMS (Supporting Information).

$[^{99m}Tc(CN3DG)_6]^+$ and $[^{99m}Tc(CO)_3(CN3DG)_3]^+$ were obtained in high radiochemical purity (>95%) verified by HPLC with the retention time 9.71 and 10.48 min (Figure 2). Under the same conditions, the retention time of $^{99m}TcO_4^-$ and $[^{99m}Tc(CO)_3(H_2O)_3]^+$ were 3.93 and 12.17 min, respectively. The specific radioactivity

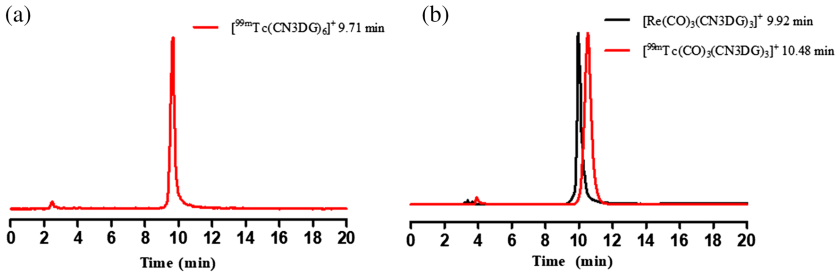

FIGURE 2 (a) HPLC profiles of $[^{99m}Tc(CN3DG)_6]^+$ and (b) co-injection HPLC profiles of $[Re(CO)_3(CN3DG)_3]^+$ and $[^{99m}Tc(CO)_3(CN3DG)_3]^+$

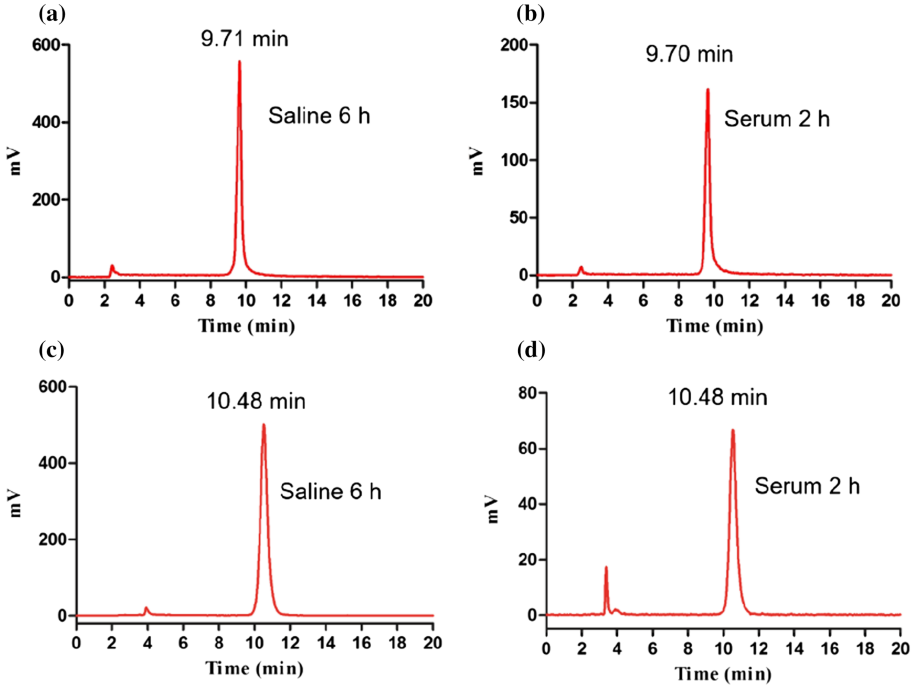

FIGURE 3 Stability studies of (a,b) $[^{99m}Tc(CN3DG)_6]^+$ and (c,d) $[^{99m}Tc(CO)_3(CN3DG)_3]^+$ in vitro

for the probes was 10.14–101.37 GBq $mmol^{-1}$. In order to confirm the chemical structure of $[^{99m}Tc(CO)_3(CN3DG)_3]^+$, the corresponding Re coordinated complex was synthesized and confirmed by ^{1}H-NMR, IR, and HRMS (Supporting Information). As shown in Figure 2, the HPLC retention time of $[^{99m}Tc(CO)_3(CN3DG)_3]^+$ (10.48 min) matched with that of $[Re(CO)_3(CN3DG)_3]^+$ (9.92 min), suggesting $[^{99m}Tc(CO)_3(CN3DG)_3]^+$ had similar structure with $[Re(CO)_3(CN3DG)_3]^+$ as shown in Figure 2b. We tried to prepare $[Re(CN3DG)_6]^+$; unfortunately, we failed to obtain the pure Re complex. The proposed structure of $[^{99m}Tc(CN3DG)_6]^+$ was shown in Figure 1b, which was similar to that of ^{99m}Tc-CN5DG as shown in Figure 1a.

3.2 | In vitro stability and the water/octanol partition coefficients studies

Both $[^{99m}Tc(CN3DG)_6]^+$ and $[^{99m}Tc(CO)_3(CN3DG)_3]^+$ were stable in saline for 6 h and in mice serum for 2 h examined by HPLC shown in Figure 3. The partition coefficients (Log P) of $[^{99m}Tc(CN3DG)_6]^+$ and $[^{99m}Tc(CO)_3(CN3DG)_3]^+$ were -4.01 ± 0.17 and -2.65 ± 0.20, demonstrating both tracers were hydrophilic. Moreover, $[^{99m}Tc(CN3DG)_6]^+$ was more hydrophilic than $[^{99m}Tc(CO)_3(CN3DG)_3]^+$, possibly because $[^{99m}Tc(CN3DG)_6]^+$ had a structure with six CN3DG ligands whereas $[^{99m}Tc(CO)_3(CN3DG)_3]^+$ had only three CN3DG ligands.

3.3 | Cell uptake studies

As shown in Figure 4, 2-mg D-glucose could significantly block the uptake value of $[^{99m}Tc(CN3DG)_6]^+$ and $[^{99m}Tc(CO)_3(CN3DG)_3]^+$ in S180 tumor cells after 4-h co-incubation, whereas 2-mg L-glucose had little affects. These findings suggested that the two complexes could be transported into S180 cells by glucose transporters.

3.4 | Biodistribution studies

The biodistribution data of $[^{99m}Tc(CN3DG)_6]^+$ and $[^{99m}Tc(CO)_3(CN3DG)_3]^+$ in S180 tumor-bearing mice

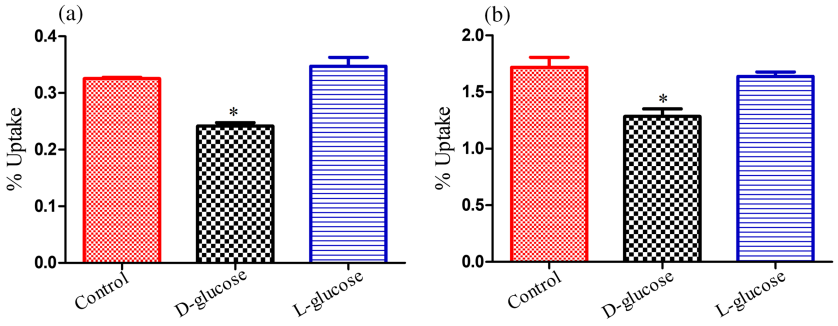

FIGURE 4 Cell uptake data of (a) $[^{99m}Tc(CN3DG)_6]^+$ and (b) $[^{99m}Tc(CO)_3(CN3DG)_3]^+$ in S180 cells after co-incubation with D-glucose or L-glucose for 4 h in vitro. $^*P < 0.05$

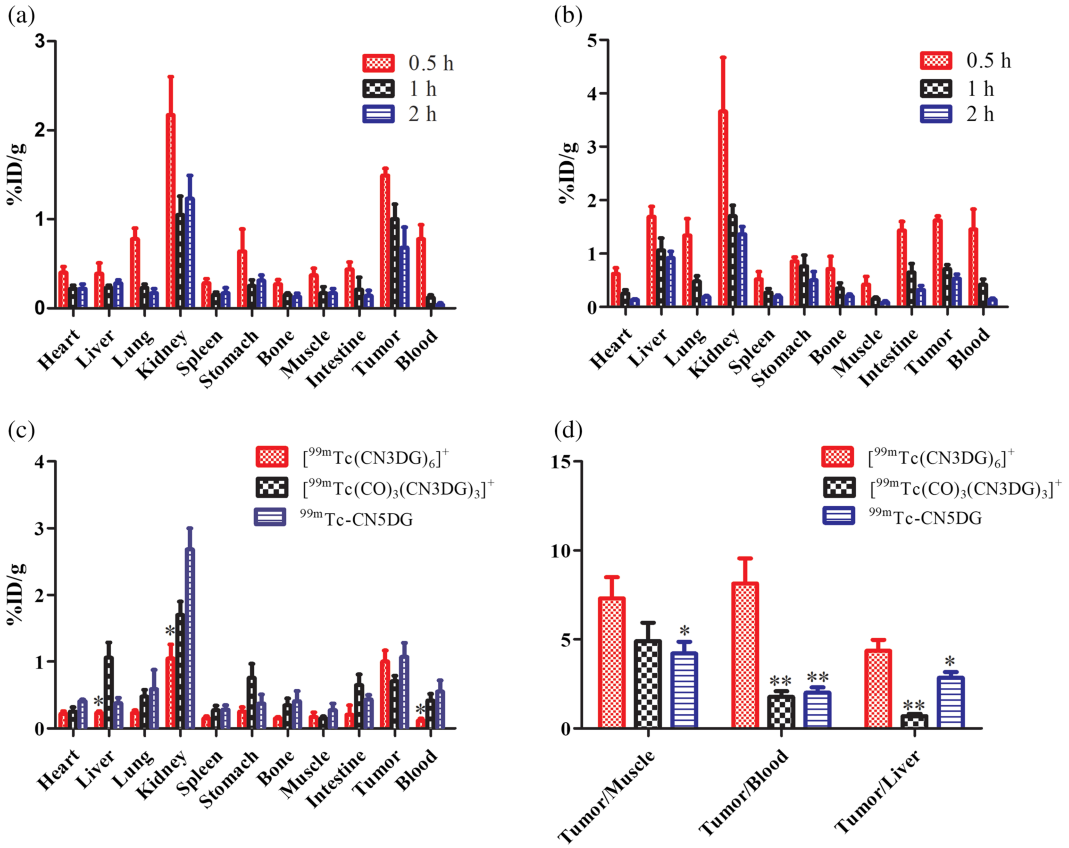

FIGURE 5 Biodistribution data of (a) $[^{99m}Tc(CN3DG)_6]^+$ and (b) $[^{99m}Tc(CO)_3(CN3DG)_3]^+$. (c) Comparison of biodistribution data of $[^{99m}Tc(CN3DG)_6]^+$, $[^{99m}Tc(CO)_3(CN3DG)_3]^+$, and ^{99m}Tc-CN5DG. (d) Comparison of the tumor/muscle, tumor/blood, and tumor/liver ratios of $[^{99m}Tc(CN3DG)_6]^+$, $[^{99m}Tc(CO)_3(CN3DG)_3]^+$, and ^{99m}Tc-CN5DG. $^*P < 0.05$, $^{**}P < 0.01$

were shown in Figure 5a,b. Both complexes had a high tumor uptake at 30 min post injection and decreased as a function of time. The highest uptake tissue for both tracers was kidney, suggesting the key clearance route was through urinary tract.

By comparison, $[^{99m}Tc(CN3DG)_6]^+$ had a slightly higher tumor uptake and lower liver and blood uptakes, resulting in higher tumor/blood and tumor/liver ratios. These differences may attribute to their different chemical structures and lipophilicity. $[^{99m}Tc(CN3DG)_6]^+$ had six CN3DG ligands and was more hydrophilic thus making its lower liver uptake (1 h after injection, 0.23 ± 0.03%ID g^{-1} vs. 1.06 ± 0.23%ID g^{-1}, $^*P < 0.05$) and blood uptake (1 h after injection, 0.12 ± 0.03%ID g^{-1} vs. 0.42 ± 0.10%ID g^{-1}, $^*P < 0.05$). Low uptake in stomach for both tracers demonstrated that they were stable in vivo.

Compared with the biodistribution data of ^{99m}Tc-CN5DG at 1 h post injection, $[^{99m}Tc(CN3DG)_6]^+$ had lower muscle uptake (0.27 ± 0.10%ID g^{-1} for ^{99m}Tc-CN5DG vs. 0.17 ± 0.07%ID g^{-1} for $[^{99m}Tc(CN3DG)_6]^+$) and blood uptake (0.55 ± 0.17%ID g^{-1} for ^{99m}Tc-CN5DG vs. 0.12 ± 0.03%ID g^{-1} for $[^{99m}Tc(CN3DG)_6]^+$) whereas the tumor uptake (1.07 ± 0.21%ID g^{-1} for ^{99m}Tc-CN5DG

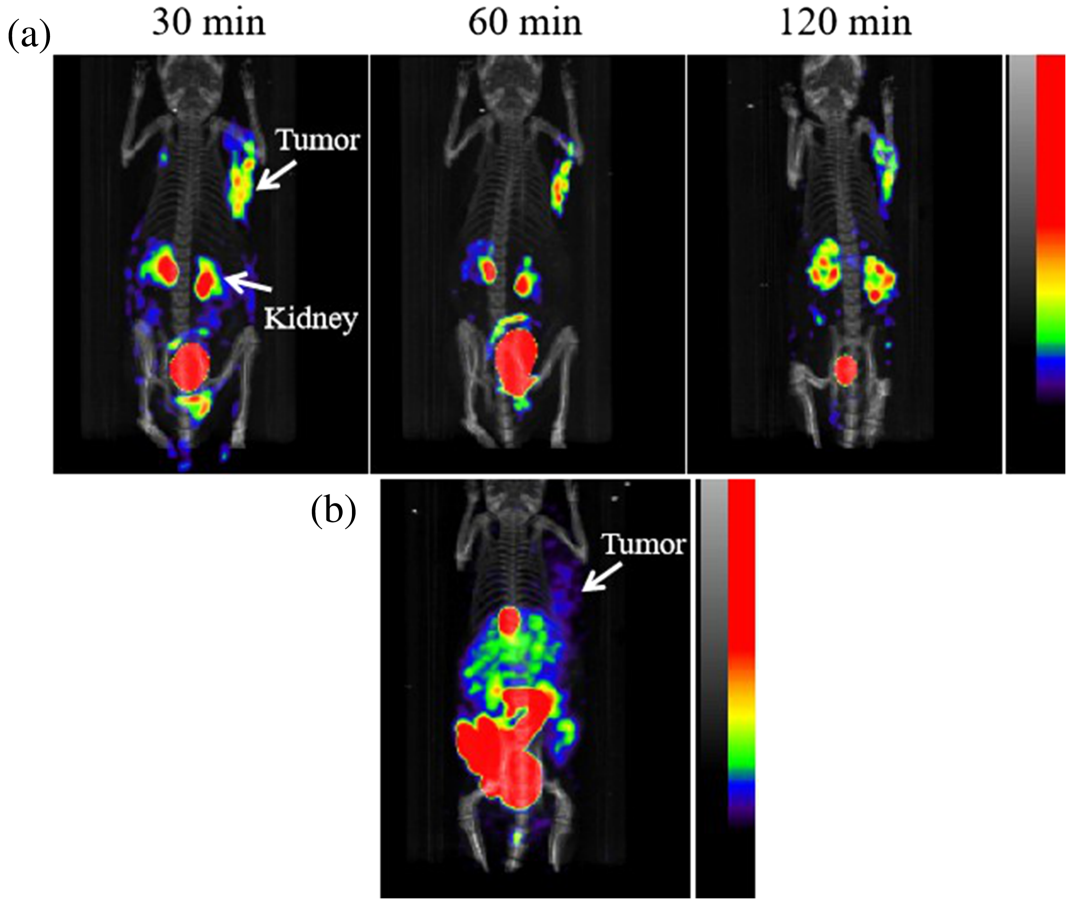

FIGURE 6 Whole body single-photon emission computed tomography (SPECT)/CT images of (a) $[^{99m}Tc(CN3DG)_6]^+$ and (b) $[^{99m}Tc(CO)_3(CN3DG)_3]^+$ in S180 tumor-bearing mice ($n = 3$)

vs. 1.00 ± 0.17%ID g^{-1} for $[^{99m}Tc(CN3DG)_6]^+$) of both had no significant difference (Figure 5c). The tumor/muscle, tumor/blood, and tumor/liver ratios of $[^{99m}Tc(CN3DG)_6]^+$ (7.31 ± 1.18, 8.14 ± 1.41, and 4.36 ± 0.62) were higher than those of ^{99m}Tc-CN5DG (4.21 ± 0.66, 2.00 ± 0.31, and 2.84 ± 0.33) (Figure 5d). This may attribute to the shorter carbon chain in the structure of CN3DG, thus causing $[^{99m}Tc(CN3DG)_6]^+$ more hydrophilic (Log P = −4.01 ± 0.17) than ^{99m}Tc-CN5DG (Log P = −3.57 ± 0.35).

3.5 | SPECT/CT imaging studies

SPECT/CT scans of S180 tumor-bearing mice were taken with $[^{99m}Tc(CN3DG)_6]^+$ (at 30, 60, and 120 min post injection; Figure 6a) and $[^{99m}Tc(CO)_3(CN3DG)_3]^+$ (at 60 min post injection; Figure 6b) using a small animal SPECT/CT scanner. As for $[^{99m}Tc(CN3DG)_6]^+$, S180 tumors could be clearly seen from the images from 30 to 120 min after injection, and there were also high uptakes in kidney and bladder. S180 tumor could also be seen from the SPECT/CT images of $[^{99m}Tc(CO)_3(CN3DG)_3]^+$ at 60 min post injection, but there were also higher uptakes in gallbladder, liver, kidney, intestine, and bladder. From the SPECT images, the region of interest (ROI) ratios of the tumor site versus corresponding nontumor site for $[^{99m}Tc(CN3DG)_6]^+$ and $[^{99m}Tc(CO)_3(CN3DG)_3]^+$ were 6.54 ± 0.42 and 4.23 ± 0.94, respectively. These results were in accordance with their biodistribution data. It is reasonable to conclude that $[^{99m}Tc(CN3DG)_6]^+$ is more suitable for tumor detection than $[^{99m}Tc(CO)_3(CN3DG)_3]^+$, and it will be a promising candidate as a tumor imaging agent.

4 | CONCLUSION

In this study, a novel D-glucosamine isocyanide (CN3DG) is synthesized and radiolabeled with $[^{99m}Tc(I)]^+$ and $[^{99m}Tc(CO)_3]^+$ to produce $[^{99m}Tc(CN3DG)_6]^+$ and $[^{99m}Tc(CO)_3(CN3DG)_3]^+$ in high radiochemical purity. Both of the tracers are stable in saline and mice serum in vitro. Cell uptake studies demonstrate that the two complexes can be transported into cells through glucose transporters. Both tracers have high tumor uptake in S180

tumor-bearing mice, and $[^{99m}Tc(CN3DG)_6]^+$ is superior to $[^{99m}Tc(CO)_3(CN3DG)_3]^+$. SPECT/CT studies demonstrate that $[^{99m}Tc(CN3DG)_6]^+$ exhibits an obvious accumulation in tumor sites and high target/nontarget ratios, suggesting it is a promising tumor imaging agent.

ACKNOWLEDGMENTS

This work is financially supported, in part, by the National Natural Science Foundation of China (21771023), the project of the Beijing Municipal Science and Technology Commission (Z181100002218033), and China Postdoctoral Science Foundation (212400211).

AUTHOR CONTRIBUTIONS

Xuran Zhang: Conceptualization; investigation. **Qianqian Gan:** Investigation. **Qing Ruan:** Investigation. **Di Xiao:** Investigation. **JunBo Zhang:** Conceptualization; funding acquisition.

DATA AVAILABILITY STATEMENT

The data that support the findings of this study are available from the corresponding author upon reasonable request.

ORCID

Xuran Zhang https://orcid.org/0000-0002-1873-936X
Junbo Zhang https://orcid.org/0000-0003-3549-6483

REFERENCES

[1] R. Bar-Shalom, A. Y. Valdivia, M. D. Blaufox, *Semin. Nucl. Med.* **2000**, *30*, 150.
[2] P. Brugarolas, J. Comstock, D. W. Dick, T. Ellmer, J. W. Engle, S. E. Lapi, S. H. Liang, E. E. Parent, N. V. Pillarsetty, S. Selivanova, X. Sun, *J. Nucl. Med. Technol.* **2020**, *48*, 34S.
[3] T. Fujiwara, K. Kubota, T. Sato, T. Matsuzawa, M. Tada, R. Iwata, M. Itoh, J. Hatazawa, K. Sato, H. Fukuda, *J. Nucl. Med.* **1990**, *31*, 1654.
[4] S. S. Gambhir, *Nat. Rev. Cancer* **2002**, *2*, 683.
[5] O. Humbert, M. Lasserre, A. Bertaut, P. Fumoleau, C. Coutant, F. Brunotte, A. Cochet, *J. Nucl. Med.* **2018**, *59*, 1035.
[6] A. van Berkel, D. Vriens, E. P. Visser, M. J. R. Janssen, M. Gotthardt, A. R. M. M. Hermus, L. F. Geus-Oei, H. J. L. M. Timmers, *J. Nucl. Med.* **2019**, *60*, 745.
[7] A. L. Branco de Barros, V. N. Cardoso, L. G. Mota, E. A. Leite, M. C. de Oliveira, R. J. Alves, *Bioorg. Med. Chem. Lett.* **2009**, *19*, 2497.
[8] X. Chen, L. Li, F. Liu, B. Liu, *Bioorg. Med. Chem. Lett.* **2006**, *16*, 5503.
[9] R. Dapueto, R. Castelli, M. Fernandez, J. A. Chabalgoity, M. Moreno, J. P. Gambini, P. Cabral, W. Porcal, *Bioorg. Med. Chem. Lett.* **2011**, *21*, 7102.
[10] J. Ding, H. Su, F. Wang, T. Chu, *Bioorg. Med. Chem. Lett.* **2019**, *29*, 1791.
[11] H. Feng, X. Wang, J. Chen, J. Cui, T. Gao, Y. Gao, W. Zeng, *Contrast Media Mol. Imaging* **2019**. 7954854/1–7954854/12
[12] J. Liang, Y. Chen, Z. Huang, Y. Zhao, L. He, *Cancer Biother. Radiopharm.* **2008**, *23*, 363.
[13] T. Liu, Q. Gan, J. Zhang, *Chem. Biol. Drug des.* **2017**, *89*, 277.
[14] T. Liu, Q. Gan, J. Zhang, Z. Jin, W. Zhang, Y. Zhang, *Med. Chem. Commun.* **2016**, *7*, 1381.
[15] T. Liu, J. Zhang, X. Wang, J. Yang, Z. Tang, J. Lu, *Curr. Med. Chem.* **2014**, *21*, 24.
[16] S. J. Oh, J.-S. Ryu, E.-J. Yoon, M. S. Bae, S. J. Choi, K. B. Park, D. H. Moon, *Appl. Radiat. Isot.* **2006**, *64*, 207.
[17] S. Singh, S. Singh, R. K. Sharma, A. Kaul, R. Mathur, S. Tomar, R. Varshney, A. K. Mishra, *New J. Chem.* **2020**, *44*, 3062.
[18] D. Dai, F. David Rollo, J. Bryant, K. E. Edmund, *Contrast Media Mol. Imaging* **2018**. 8969714/1–8969714/9
[19] N. R. Schechter, W. D. Erwin, D. J. Yang, E. E. Kim, R. F. Munden, K. Forster, L. C. Taing, J. D. Cox, H. A. Macapinlac, D. A. Podoloff, *Eur. J. Nucl. Med. Mol. Imaging* **2009**, *36*, 1583.
[20] D. J. Yang, C.-G. Kim, N. R. Schechter, A. Azhdarinia, D.-F. Yu, C.-S. Oh, J. L. Bryant, J. J. Won, E. E. Kim, D. A. Podoloff, *Radiology* **2003**, *226*, 465.
[21] X. Zhang, Q. Ruan, X. Duan, Q. Gan, X. Song, S. Fang, X. Lin, J. du, J. Zhang, *Mol. Pharmaceutics* **2018**, *15*, 3417.
[22] X. Duan, Q. Gan, X. Song, S.-A. Fang, X. Zhang, Q. Ruan, J. Zhang, *Appl. Organomet. Chem.* **2018**, *32*, e4424.
[23] M. B. Mallia, A. Mathur, R. Sharma, C. Kumar, H. D. Sarma, S. Banerjee, A. Dash, *J. Radioanal. Nucl. Chem.* **2018**, *317*, 1203.
[24] Y. Mizuno, N. Komatsu, T. Uehara, Y. Shimoda, K. Kimura, Y. Arano, H. Akizawa, *Nucl. Med. Biol.* **2020**, *86–87*, 30.
[25] Y. Mizuno, T. Uehara, H. Hanaoka, Y. Endo, C.-W. Jen, Y. Arano, *J. Med. Chem.* **2016**, *59*, 3331.
[26] Q. Ruan, X. Zhang, J. Zhang, *Appl. Organomet. Chem.* **2020**, *34*, e5798.

SUPPORTING INFORMATION

Additional supporting information may be found online in the Supporting Information section at the end of this article.

How to cite this article: Zhang X, Gan Q, Ruan Q, Xiao D, Zhang J. Evaluation and comparison of ^{99m}Tc-labeled D-glucosamine derivatives with different ^{99m}Tc cores as potential tumor imaging agents. *Appl Organomet Chem*. 2020;34:e6008. https://doi.org/10.1002/aoc.6008